NACA RM L51D26

NACA

RESEARCH MEMORANDUM

COMPARISON OF ZERO-LIFT DRAG DETERMINED BY FLIGHT TESTS AT TRANSONIC SPEEDS OF PYLON, UNDERSLUNG, AND SYMMETRICALLY MOUNTED NACELLES AT 40 PERCENT SEMISPAN OF A 45° SWEPTBACK WING AND BODY COMBINATION

By Sherwood Hoffman

Langley Aeronautical Laboratory
Langley Field, Va.

NATIONAL ADVISORY COMMITTEE
FOR AERONAUTICS

WASHINGTON

June 25, 1951

NATIONAL ADVISORY COMMITTEE FOR AERONAUTICS

RESEARCH MEMORANDUM

COMPARISON OF ZERO-LIFT DRAG DETERMINED BY FLIGHT TESTS AT TRANSONIC SPEEDS OF PYLON, UNDERSLUNG, AND SYMMETRICALLY MOUNTED NACELLES AT 40 PERCENT SEMISPAN OF A 45° SWEPTBACK WING AND BODY COMBINATION

By Sherwood Hoffman

SUMMARY

The effect on drag of varying the vertical position of a nacelle at 40 percent semispan of a 45° sweptback wing and body combination has been determined through transonic flight tests at zero lift. Three nacelle positions were investigated: a pylon mounted nacelle, an underslung nacelle, and a symmetrically mounted nacelle. The nacelle fineness ratio of 9.66 was reduced to 8.0 for pylon mounting. The nose of each nacelle was located 1.20 wing-chord lengths in front of the wing leading edge. The pylon was 6 percent thick, swept forward 68° from the wing, and was 20 percent of the local wing chord in length. The wing had an NACA 65A009 airfoil section parallel to the free stream. The fuselage fineness ratio was 10.0.

Of the three nacelle arrangements tested, the pylon-nacelle arrangement had the highest drag, particularly between Mach numbers of 0.90 and 1.0. High nacelle drags that were due to unfavorable interference occurred near a Mach number of 1 for the pylon, the underslung, and the symmetrically mounted nacelles. For the model with the pylon-nacelle arrangement, the force-break Mach number was approximately 0.90, which was 0.03 less than for the other nacelle arrangements and about 0.06 less than for the basic configuration.

INTRODUCTION

As part of a general transonic research program of the National Advisory Committee for Aeronautics, rocket-propelled models were tested in free flight to determine the effect of nacelle location on the zero-lift drag of transonic research configurations. Previous investigations

(references 1 and 2) show the effect on drag of the variations in the chordwise and spanwise location of a nacelle mounted on the wing of a transonic research vehicle. The present paper gives a comparison of the drag obtained from pylon, underslung, and symmetrically mounted nacelles located at 40 percent semispan and in a forward chordwise position. Drag data for the underslung and the symmetrically mounted nacelles were recently published as part of the investigation of reference 1.

The pylon, which was designed to have low transonic drag and a force-break Mach number above 0.9, was swept forward 68° from the wing and was 6 percent thick in the free-stream direction. A pylon length approximately equal to 20 percent of the local wing chord was selected to give low interference drag at high subsonic speeds (see reference 3). In an attempt to minimize the interference drag, the length of the nacelle used in reference 1 was reduced for pylon mounting.

Flight test at zero lift for the pylon-nacelle arrangement covered a continuous Mach number range from 0.8 to 1.13. The Reynolds number, based on wing mean aerodynamic chord, varied from 3.8×10^6 to 5.9×10^6.

SYMBOLS

b	wing span, feet
c	wing chord, inches
C_D	total drag coefficient based on S_W
C_{D_N}	drag coefficient for nacelle, pylon, and interference based on S_F
M	Mach number
p	rolling velocity, radians per second
$\frac{pb}{2V}$	wing-tip helix angle, radians
R	Reynolds number, based on wing mean aerodynamic chord
S_F	frontal area of one nacelle, square feet
S_W	total wing plan-form area, square feet
V	velocity along flight path, feet per second

x station, inches

y ordinate, inches

MODELS

Details and dimensions of the wing-body-fin combination, pylon, nacelles, and nacelle positions are given in figures 1 and 2 and tables I to IV. Photographs showing the general arrangements of the models flown are presented as figure 3.

The wing had a sweepback angle of 45° along the quarter-chord line, an aspect ratio of 6.0, a taper ratio of 0.6, and an NACA 65A009 airfoil section in the free-stream direction. The wing leading edge intersected the maximum diameter of the fuselage. The fuselage fineness ratio was 10.0. The ratio of total wing plan-form area to fuselage frontal area was 16.0.

The models with the symmetrically mounted and the underslung nacelles referred to in this paper were models D and H of reference 1. An identical wing-body-fin combination was employed for the pylon-nacelle model; however, the nacelle fineness ratio was reduced from 9.66 to 8.0 by removing a part of the nacelle cylindrical midsection. Each nacelle had an NACA 1-50-250 nose-inlet profile, a cylindrical midsection, and an afterbody of NACA 111 proportions.

The pylon was untapered and swept forward 68° from the wing. The airfoil section of the pylon, which was formed in the free-stream direction by two circular arcs of different radii, was 6 percent thick with maximum thickness at 30 percent of the pylon chord. The pylon length, minimum distance between nacelle and wing, was equal to 20 percent of the wing chord at 40 percent semispan. For the three positions investigated, nacelles were mounted in a constant chordwise position with the solid nose inlet located ahead of the wing a distance equal to 120 percent of the wing chord. The pylon and the underslung nacelles were placed on opposite surfaces of each wing (figs. 3(a) and 3(b)). This asymmetric arrangement was used so that any trim change would produce roll rather than pitch and the model would fly essentially at zero lift. To obtain an indication of the roll, a modified spinsonde transmitter (see reference 4) was installed in the fuselage nose of the pylon-nacelle model.

TESTS AND MEASUREMENTS

The models were flight-tested at the Pilotless Aircraft Research Station at Wallops Island, Va. Since the underslung and the symmetrically mounted nacelle models were tested previously, it was only required to test a pylon-nacelle model by the testing technique of reference 1. Velocity and trajectory data were obtained from the CW Doppler velocimeter and the NACA modified SCR-584 radar tracking unit. A survey of atmospheric conditions for each test was made through radiosonde measurements from an ascending balloon. The rolling velocity and resultant wing-tip helix angle $pb/2V$ for the pylon-nacelle model were determined by the method described in reference 4.

The variation of Reynolds number with Mach number for all the models tested is shown in figure 4 and varied approximately from 3.8×10^6 at $M = 0.8$ to about 7.3×10^6 at $M = 1.25$.

The magnitude of the error in drag was established from three identical models without nacelles in reference 1 and was based on the maximum deviation found between faired curves of experimental drag points. The error in the total drag coefficient, based on total wing plan-form area, was within ± 0.0004. For the nacelle-plus-interference drag coefficient, based on nacelle frontal area, the error was within ± 0.046. The estimated error for the wing-tip helix angle $pb/2V$ was ± 0.0055 radian for subsonic speeds and ± 0.0025 radian for supersonic speeds. The accuracy of the flight Mach number was approximately ± 0.005.

The definition of nacelle-plus-interference drag coefficient for the pylon-nacelle model was extended to include pylon drag and its effect on interference; however, this drag coefficient was based on nacelle frontal area to be consistent with C_{D_N} used for the underslung and the symmetrical nacelle positions. The relationship for nacelle-plus-interference drag coefficient was

$$C_{D_N} = \left(C_{D_{\text{nacelles on}}} - C_{D_{\text{nacelles off}}}\right) \frac{S_W}{2S_F}$$

The drag coefficient C_D was based on total wing plan-form area S_W.

RESULTS AND DISCUSSION

The variations of total drag coefficient with Mach number for models A, B, and C with pylon, underslung, and symmetrical nacelle installations, respectively, and for the configuration without nacelles (model D) are given in the upper chart of figure 5. Of the three models tested, the model with the pylon-nacelle arrangement had the highest drag, particularly from $M = 0.90$ and $M = 1.0$. At $M = 0.95$, the total drag coefficient of the model with the pylon-nacelle arrangement was 0.0065 greater than for either of the other two arrangements. For the configuration with the pylon-nacelle installation, the force-break Mach number was approximately 0.90, which was 0.03 less than for the other wing-body-nacelle configurations and about 0.06 less than for the basic wing-body configuration.

In the lower chart of figure 5, C_{D_N} for models A, B, and C are compared with the drag coefficient of an isolated nacelle, which was estimated in reference 1. A comparison between the estimated isolated nacelle drag and the measured nacelle drag is indicative of the interference drag except for model A, which also includes the drag of the pylon.

From the variations of C_{D_N} with M for the pylon, the underslung, and the symmetrically mounted nacelle positions, it was evident that the high nacelle drags near $M = 1$ were due to unfavorable interference. The largest interference drag, which was from the pylon-nacelle arrangement, was probably due to the nacelle location rather than the pylon. The drag of the pylon alone should have been low since the pylon was swept forward 68° and was 6 percent thick. At supersonic speeds, the nacelle drags for the three positions tested were approximately twice that estimated for the isolated nacelle.

The maximum wing-tip helix angle for the model with the pylon-nacelle arrangement was 0.023 radian (1.32°) at $M = 1.13$. For this value of $pb/2V$, the effective angle of attack at the 40-percent-semispan station (pylon-nacelle location) would be approximately 0.5°. From available data in reference 3 for a similar wing-pylon-nacelle arrangement, the drag due to lift for an angle of attack less than 1° would be negligible.

CONCLUSIONS

The effect on drag of varying the vertical position of a nacelle at 40 percent semispan of a 45° sweptback wing and body combination has

been determined through transonic flight tests at zero lift. The positions investigated were for a nacelle mounted on a sweptforward (from wing) pylon, for an underslung nacelle, and for a symmetrically mounted nacelle. The nacelle fineness ratio was reduced from 9.66 to 8.0 for pylon mounting. The following effects were noted:

1. Of the three nacelle positions tested, the pylon-nacelle arrangemany had the highest drag, particularly between Mach numbers of 0.90 and 1.0. The high nacelle drags that occurred near a Mach number of 1.0 from the pylon, the underslung, and the symmetrically mounted nacelles were due to unfavorable interference.

2. For the model with the pylon-nacelle arrangement, the force-break Mach number was approximately 0.90, which was 0.03 less than for the other wing-body-nacelle arrangements and about 0.06 less than for the basic wing-body configuration.

Langley Aeronautical Laboratory
National Advisory Committee for Aeronautics
Langley Field, Va.

REFERENCES

1. Pepper, William B., Jr., and Hoffman, Sherwood: Transonic Flight Tests to Compare the Zero-Lift Drag of Underslung and Symmetrical Nacelles Varied Chordwise at 40 Percent Semispan of a 45° Sweptback, Tapered Wing. NACA RM L50G17a, 1950.

2. Pepper, William B., Jr., and Hoffman, Sherwood: Comparison of Zero-Lift Drags Determined by Flight Tests at Transonic Speeds of Symmetrically Mounted Nacelles in Various Spanwise Positions on a 45° Sweptback Wing and Body Combination. NACA RM L51D06, 1951.

3. Spreeman, Kenneth P., and Alford, William J., Jr.: Investigation of the Effects of Geometric Changes in an Underwing Pylon-Suspended External-Store Installation on the Aerodynamic Characteristics of a 45° Sweptback Wing at High Subsonic Speeds. NACA RM L50L12, 1951.

4. Harris, Orville R.: Determination of the Rate of Roll of Pilotless Aircraft Research Models by Means of Polarized Radio Waves. NACA TN 2023, 1950.

TABLE I

FUSELAGE COORDINATES

x (in.)	y (in.)
0	0
.4	.185
.6	.238
1.0	.342
2.0	.578
4.0	.964
6.0	1.290
8.0	1.577
12.0	2.074
16.0	2.472
20.0	2.772
24.0	2.993
28.0	3.146
32.0	3.250
36.0	3.314
40.0	3.334
44.0	3.304
48.0	3.219
52.0	3.037
56.0	2.849
60.0	2.661
64.0	2.474
66.7	2.347

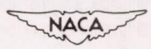

TABLE II

COORDINATES OF THE NACA 65A009 AIRFOIL

x/c (percent)	y/c (percent)
0	0
.5	.688
.75	.835
1.25	1.065
2.5	1.460
5.0	1.964
7.5	2.385
10.0	2.736
15.0	3.292
20.0	3.714
25.0	4.036
30.0	4.268
35.0	4.421
40.0	4.495
45.0	4.485
50.0	4.377
55.0	4.169
60.0	3.874
65.0	3.509
70.0	3.089
75.0	2.620
80.0	2.117
85.0	1.594
90.0	1.069
95.0	.544
100.0	.019
Leading-edge radius, 0.58 percent c	

TABLE III

COORDINATES FOR SOLID NACELLE

x (in.)	y (in.)
0	0
.100	.070
.330	.169
.830	.336
1.330	.489
1.830	.622
2.330	.747
2.580	.800
2.958	.876
3.585	.974
4.840	1.105
6.095	1.190
7.350	1.240
8.605	1.255
16.830	1.255
17.872	1.237
18.913	1.195
19.955	1.127
20.996	1.029
22.038	.909
23.079	.768
24.121	.616
24.250	.598

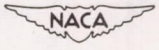

TABLE IV

COORDINATES FOR PYLON SECTION

[Free-stream direction]

x (in.)	y (in.)
0	0
.50	.091
1.00	.163
1.50	.217
2.00	.242
2.70	.270
3.50	.265
4.00	.258
5.00	.223
6.00	.196
7.00	.144
8.00	.072
8.50	.041
9.00	.000

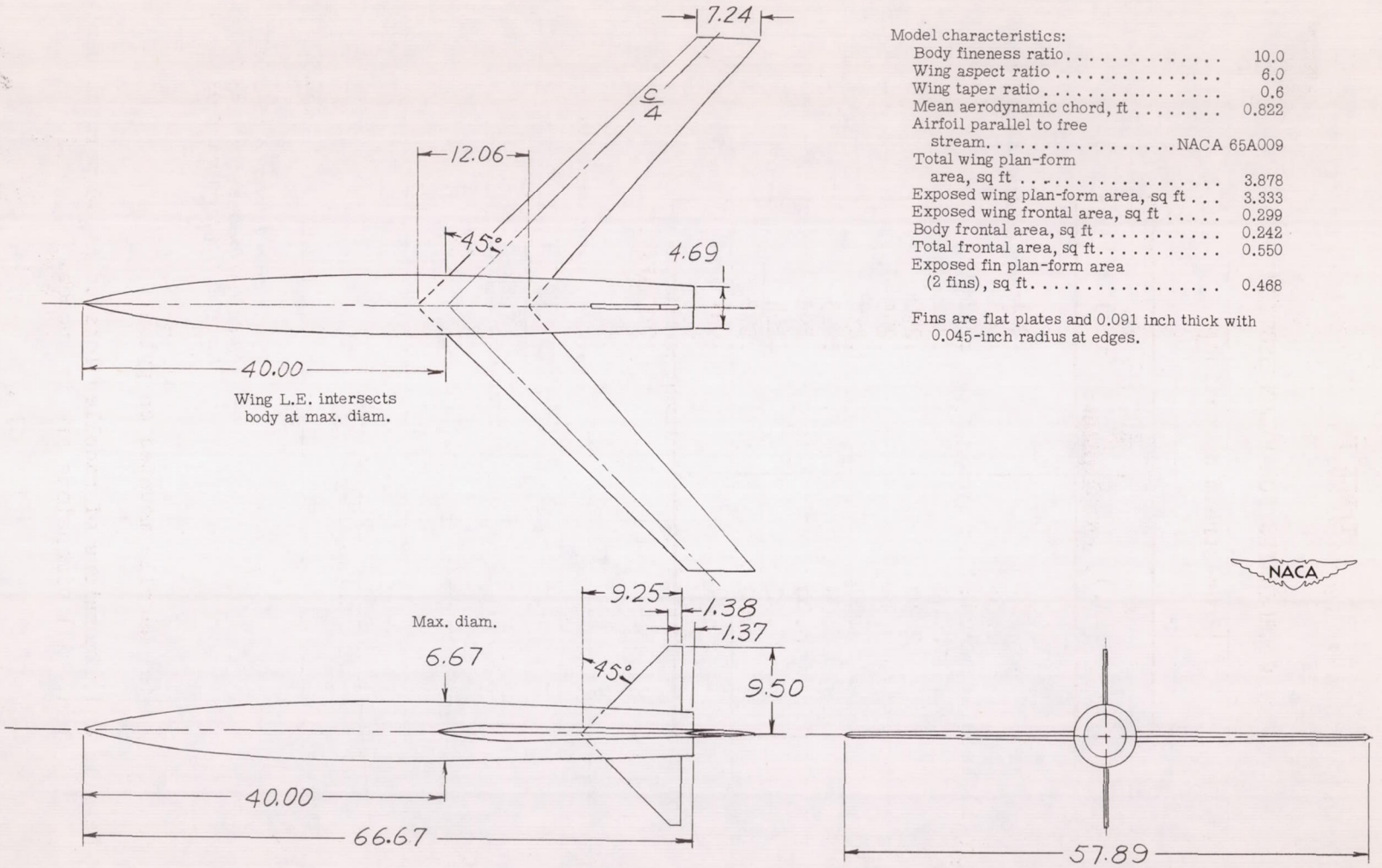

Model characteristics:

Body fineness ratio	10.0
Wing aspect ratio	6.0
Wing taper ratio	0.6
Mean aerodynamic chord, ft	0.822
Airfoil parallel to free stream	NACA 65A009
Total wing plan-form area, sq ft	3.878
Exposed wing plan-form area, sq ft	3.333
Exposed wing frontal area, sq ft	0.299
Body frontal area, sq ft	0.242
Total frontal area, sq ft	0.550
Exposed fin plan-form area (2 fins), sq ft	0.468

Fins are flat plates and 0.091 inch thick with 0.045-inch radius at edges.

Figure 1.- General arrangement and dimensions of test model. All dimensions are in inches.

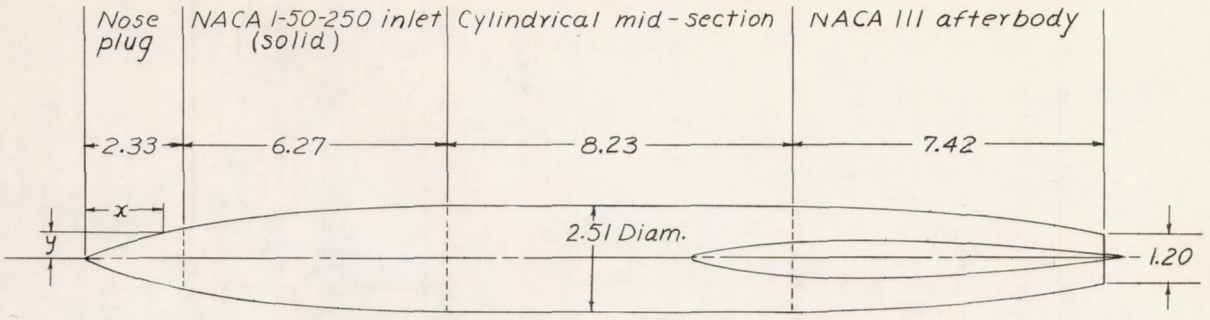

(a) Nacelle mounted in symmetrical position.

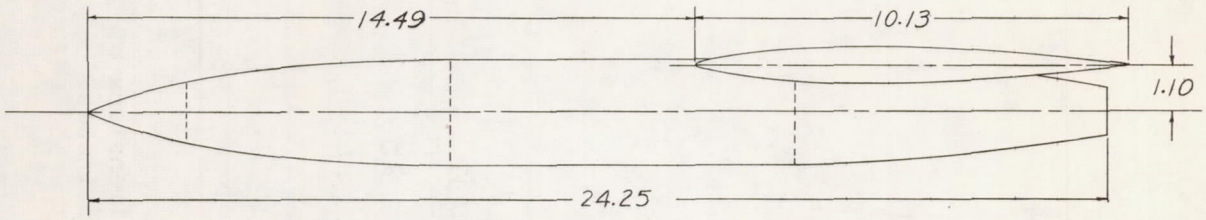

(b) Nacelle mounted in underslung position.

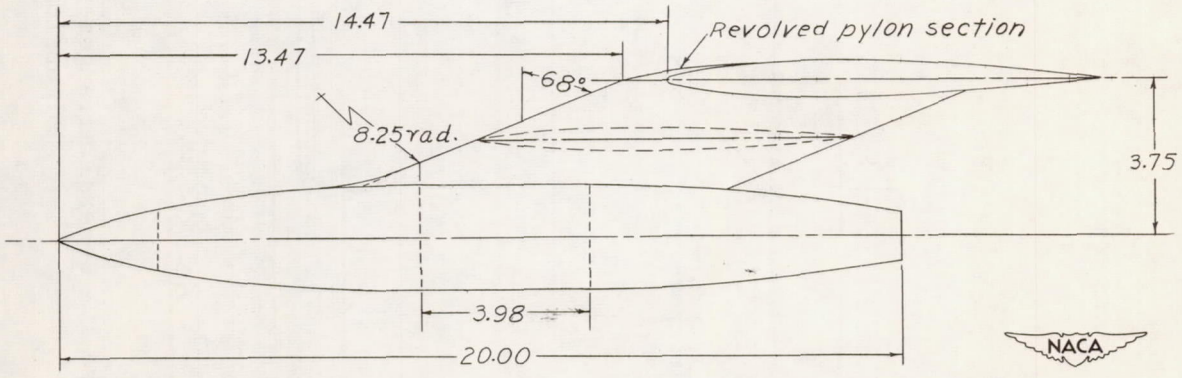

(c) Nacelle mounted on pylon.

Figure 2.- Details and dimensions of nacelles located at 40 percent semi-span. All dimensions are in inches.

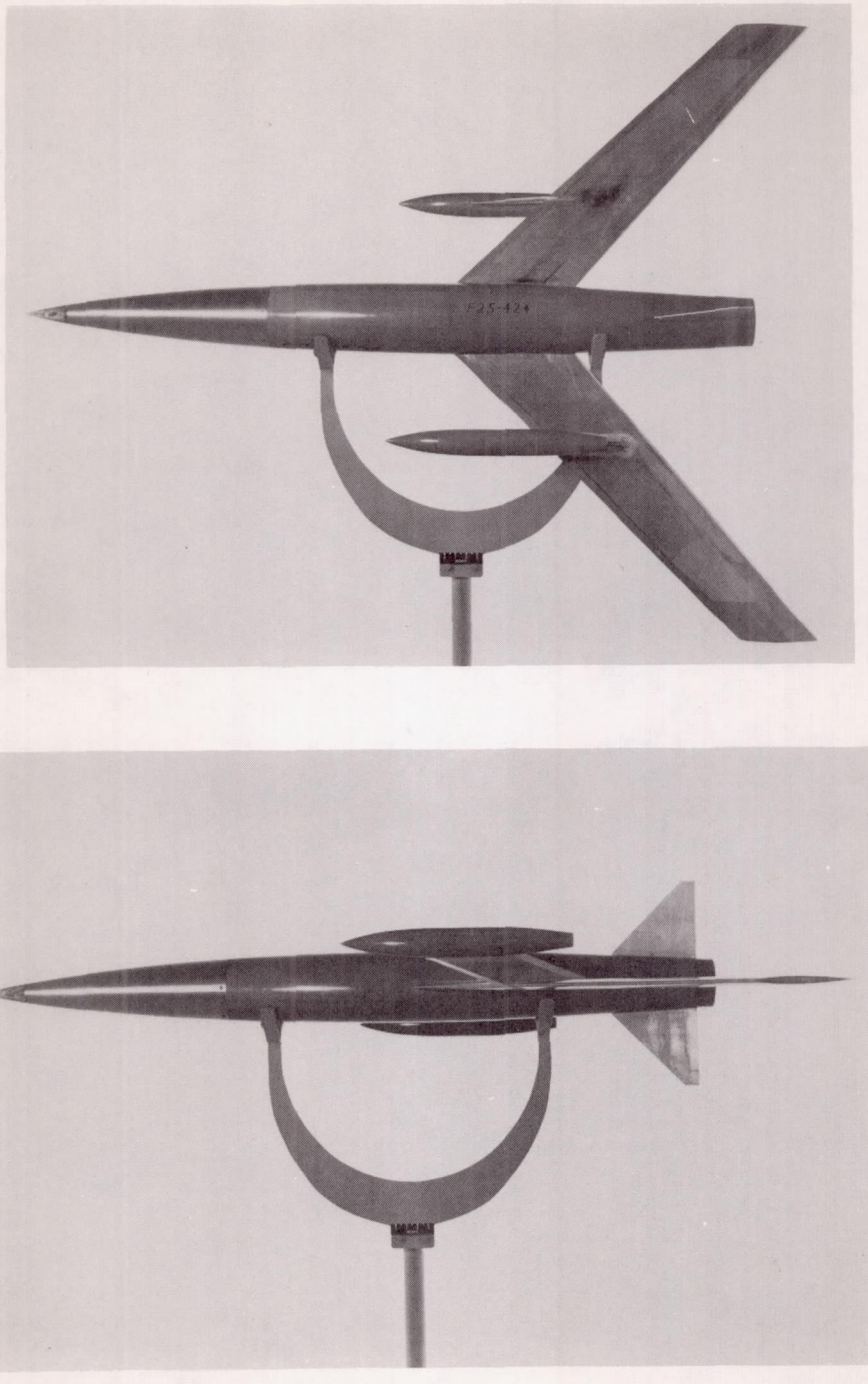

(a) Model with pylon-nacelle installation.

NACA L-69128

Figure 3.- General views of test models.

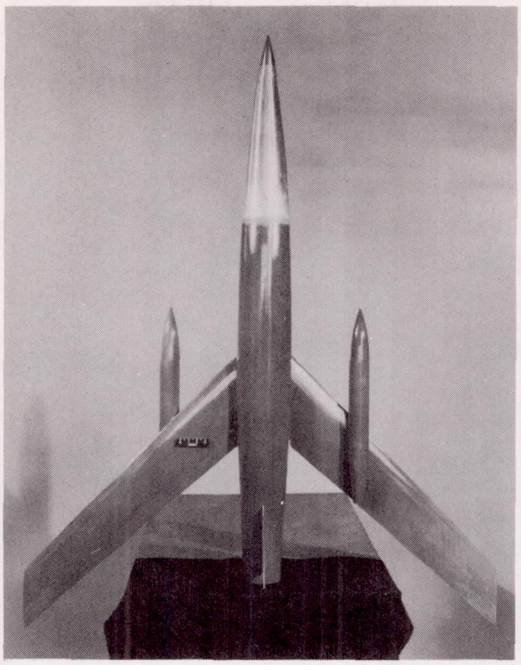

(b) Model with underslung nacelles.

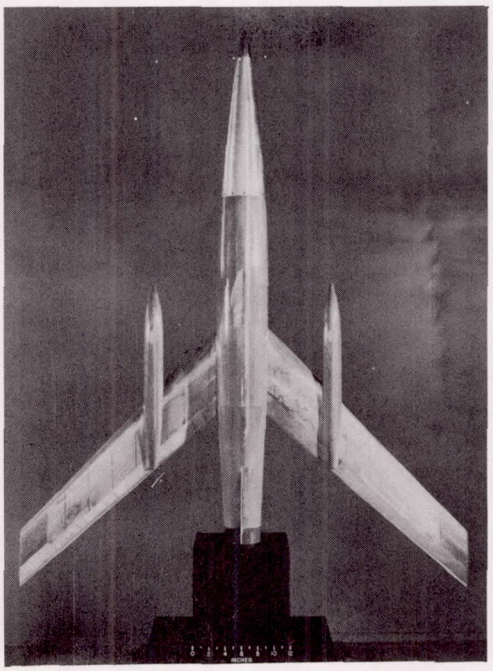

(c) Model with symmetrically mounted nacelles.

NACA

L-69129

Figure 3.- Concluded.

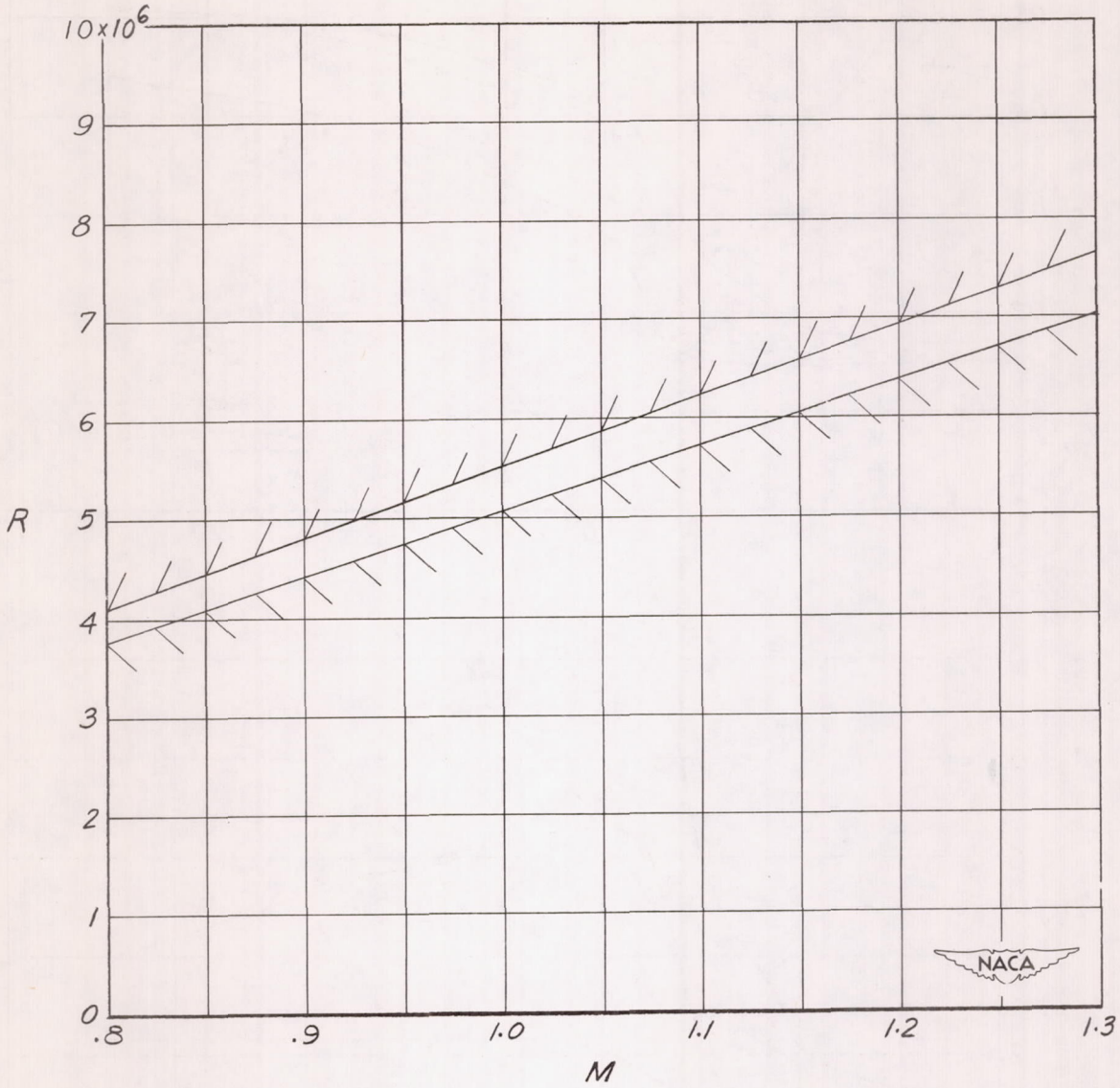

Figure 4.- Variation of Reynolds number with Mach number for models tested. Reynolds number based on wing mean aerodynamic chord.

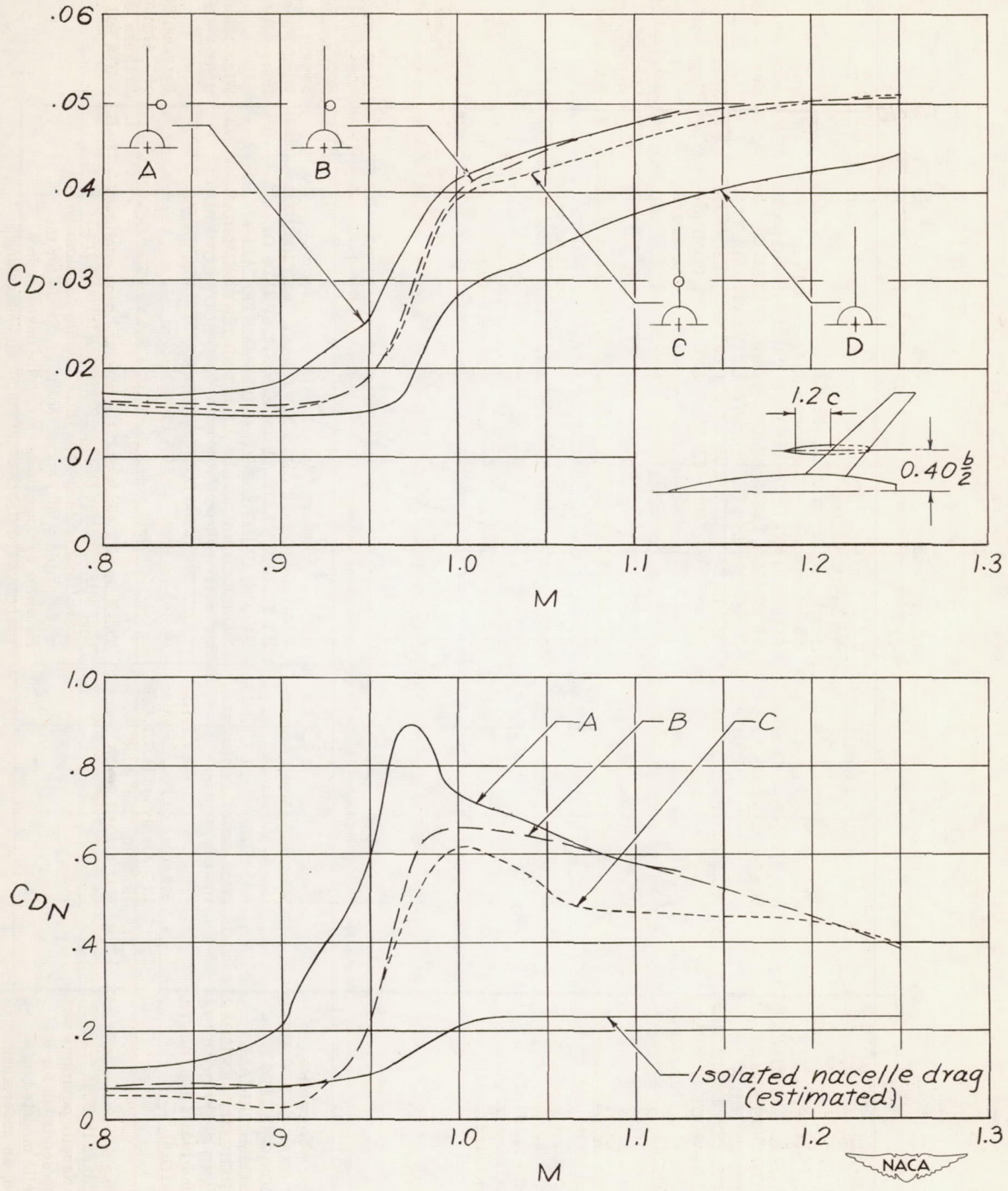

Figure 5.- Variations of total and nacelle-plus-interference drag coefficients with Mach number.